Computers & Structures Vol. 20, No. 5, pp. 877–883, 1985
Printed in Great Britain.

0045-7949/85 $3.00 + .00
Pergamon Press Ltd.

MACRO-ELEMENT ANALYSIS

THOMAS J. PARSONS†
National Institute for Occupational Safety and Health, Morgantown, West Virginia, U.S.A.

HOTA V. S. GANGARAO‡
Department of Civil Engineering, West Virginia University, Morgantown, West Virginia, U.S.A.

and

WILLIAM C. PETERSON§
General Electric Co., Space Division, King of Prussia, Pennsylvania, U.S.A.

(*Received* 30 *November* 1983; *received for publication* 19 *January* 1984)

Abstract—In recent years methods of analyzing plates in bending via large or macro-element have been studied. Herein, a method of studying plate behavior by a macro-flexibility approach is introduced. Deflected shapes of macro-elements of rectangular shapes were obtained by a shape function that satisfies all four boundary conditions and the bi-harmonic equation. The shape functions were a sum of sinusoidal and polynomial terms with undetermined coefficients. The elements that satisfy moment and shear conditions, were assembled by utilizing compatibility equations for deflection and slope. This resulted in equilibrium of forces and moments for all lines along the common edges of macro-elements. Three bounded domains were analyzed, and the results were compared to solutions obtained from classical and finite element methods. The convergence of the macro-approach was checked by progressively increasing the number of harmonics. The study of the numerical results indicates that excellent results can be obtained within the first three harmonics.

By minimizing the number of elements used to model a domain, the computational efficiency of plate analysis can be improved and inversion errors can be minimized. One way to accomplish this is to utilize elements of maximum size possible in the model without losing the accuracy. These elements are referred to herein as macro-elements. These elements should satisfy as many boundary conditions as possible, if not all four conditions. Also, the accuracy of the model should be independent of the number of elements in the model.

The efforts of Gutkowski[6, 7] and Wah[10] have demonstrated the macro-approach. Gutkowski advanced the art of introducing the "Finite Panel Method" (FPM). This approach "offers an approximate, multi, degree-of-freedom approach for analyzing continuous rectangular, isotropic plate system"[6]. Gutkowski used Levy type displacement functions (shape functions) that advanced the finite strip approach to an array of orthotropic, rectangular panels that are continuous over rigid supports. The shape function is used for the development of an 8 degree-of-freedom stiffness matrix. The mathematical model of the bounded domain is formed by the construction of a global stiffness matrix from the shape functions. Continuity of moment and deflection is satisfied along the node lines.

Wah proposed an approach to solving elastic quadrilateral plates by a "combination of analytical procedures and solution based on least squares"[10]. The method, partitions a quadrilateral plate into two triangles which are joined by writing continuity (compatibility) equations.

†Civil Engineer.
‡Professor.
§Senior Analyst.

The triangle's deflection is represented by:

$$W = W_c + W_p \tag{1}$$

where "W_c is the sum of any desired number of terms of the eigenfunctions each of which is multiplied by an arbitrary constant, and W_p is the appropriate particular integral"[10]. The particular integral satisfies the biharmonic equation for the given boundary conditions.

The deflection equation, (1), is satisfied along the common edges of the triangles. Continuity equations for deflection, slope, moment, and shear are written at a set of points along the continuity line. The unknown coefficients produced by the continuity equations are determined by using a least squares and collocation method.

GangaRao[4], GangaRao and Chaudhary[1] and Farran[2] have developed a macro-approach for the modeling of beams and plates. GangaRao and Chaudhary developed macro-elements that have polynomial shape functions for skewed and triangular plates with fixed and simply supported boundaries. Farran expanded their approach for anisotropic plates by replacing the boundaries with edge beams.

METHODOLOGY

The macro-approach being presented herein models the domain with the domain's boundary conditions and the elements' boundary conditions coterminous at as many points as possible. The elements' boundaries that form partition lines within the domain are modeled as free boundaries. By forcing deflection and slope compatibility between adjacent elements (common edge), it is possible to determine the assembled elements' deflection, slope, and mo-

ment at any point in the domain. The compatibility equations equate the slope and deflection at each point along the common edges, thus, permitting the determination of the deflection, slope, moment, and shear values anywhere within the domain or on the boundary[8].

To develop macro-elements that are independent of the number of elements within the domain, the element's shape function is chosen in the form of a series. Therefore, the function's accuracy is dependent on the number of terms in the series, not on the number of nodes, as in the finite element or the finite difference approach.

A general shape function is formulated by modifying the Navier solution to the plate bending problem. This is accomplished by adding polynomial terms with undetermined coefficients. The polynomial terms and the Fourier coefficients are determined by the boundary conditions and the biharmonic equation. The shape function is represented by:

$$w(x,y) = \sum_{i=1}^{x}\sum_{j=1}^{x} W_{ij}\sin\left(\frac{i\pi x}{a}\right)\sin\left(\frac{j\pi y}{b}\right) + \sum_{i=1}^{x}\sin\left(\frac{i\pi x}{a}\right)(C_i^1 y^3 + C_i^2 y^2 + C_i^3 y + C_i^4) + \sum_{j=1}^{x}\sin\left(\frac{j\pi y}{b}\right)(C_j^5 x^3 + C_j^6 x^2 + C_j^7 x + C_j^8) \quad (2)$$

where a is the x dimension of the element; b is the y dimension of the element; and w_{ij}, c_k^n are the unknown coefficients.

ASSEMBLAGE OF THE MACRO-ELEMENTS

To determine the forces and displacements within the domain, the macro-elements are assembled using equilibrium and compatibility equations. One step in assembling the elements is to determine the interactive forces (moments and forces) needed to define the assembled domain. These forces are determined by a system of compatibility equations that equate the element's slopes and deflection along the common edge.

The shear forces and moments along the common edges are determined by writing two compatibility equations per edge—one equating the deflection between adjacent elements, and the other equating the slopes. The deflection equation is composed of three parts (Fig. 1): (1) deflection at a common edge produced by the arbitrary loading, (2) deflection at the common edge produced by a unit point load, and (3) deflection at the common edge produced by a unit point moment. To solve for the interactive forces, the unit point load and moment are multiplied by an edge load and an edge moment of arbitrary magnitude. The magnitudes of the arbitrary edge load and moment are determined through a system of compatibility equations.

A unit point load and moment are placed along the common edge by modifying the boundary conditions. To obtain the moment at the free edge, the moment boundary condition is set equal to a unit point moment. The moment parallel to the x axis is expressed as:

$$\frac{\partial^2 w(x,y)}{\partial x^2} + \nu\frac{\partial^2 w(x,y)}{\partial y^2} = \frac{\delta(y-\eta)}{D} \quad (3)$$

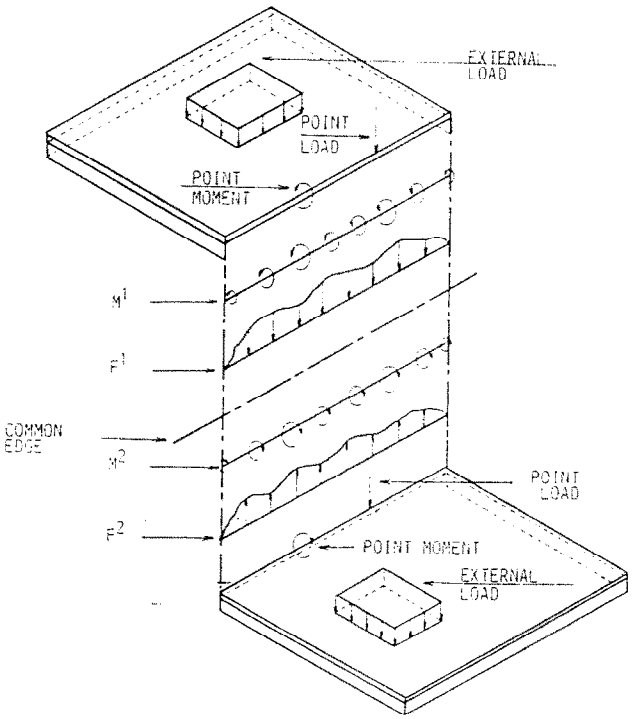

Fig. 1. The common edge forces.

and the moment along the y axis is expressed as:

$$\frac{\partial^2 w(x,y)}{\partial y^2} + v\frac{\partial^2 w(x,y)}{\partial x^2} = \frac{\delta(x-\xi)}{D} \tag{4}$$

where: v is Poison's ratio; η is the y coordinate of the point load or moment; ξ is the x coordinate of the point load or moment; and δ is the delta operator.

The unit point load is obtained by setting the force along the free edge equal to a unit load. The point load at the edge parallel to the x axis is expressed as:

$$\frac{\partial^3 w(x,y)}{\partial x^3} + (2-v)\frac{\partial^3 w(x,y)}{\partial y^2 \partial x} = \frac{\delta(y-\eta)}{D} \tag{5}$$

and as:

$$\frac{\partial^3 w(x,y)}{\partial y^3} + (2-v)\frac{\partial^3 w(x,y)}{\partial x^2 \partial y} = \frac{\delta(x-\epsilon)}{D} \tag{6}$$

when parallel to the y axis.

The δ term is expressed in series form as:

$$\delta(x-\xi) = \sum_{i=1}^{\infty} \frac{2}{aD}\sin\left(\frac{i\pi\xi}{a}\right)\sin\left(\frac{i\pi x}{a}\right) \tag{7}$$

in the x direction;
and

$$\delta(y-\eta) = \sum_{i=1}^{\infty} \frac{2}{bD}\sin\left(\frac{j\pi\eta}{b}\right)\sin\left(\frac{j\pi y}{b}\right) \tag{8}$$

in the y direction; where a is the x dimension of the element; and b is the y dimension of the element.

The compatibility equations for deflection and slope are written in the following manner for a domain modeled with two elements.

$$\triangle^{al} + F^1\triangle^{pl} + M^1\triangle^{pm} = \triangle^{al} + F^2\triangle^{pl} + M^2\triangle^{pm} \tag{9}$$

$$\bigcirc^{al} + F^1\bigcirc^{pl} + M^1\bigcirc^{pm} = \bigcirc^{al} + F^2\bigcirc^{pl} + M^2\bigcirc^{pm} \tag{10}$$

where $\triangle^{al}$ is the deflection produced by the arbitrary external loading along the common edge; $\triangle^{pl}$ is the deflection produced by the unit point load along the common edge; $\triangle^{pm}$ is the deflection produced by the unit point moment along the common edge; $\bigcirc^{al}$ is the slope produced by the arbitrary loading along the common edge; $\bigcirc^{pl}$ is the slope produced by the unit point load along the common edge; $\bigcirc^{pm}$ is the slope produced by the unit point moment along the common edge; $F^1 = F^2$ the edge load of arbitrary value along the common edge; and, $M^1 = M^2$ the edge moment of arbitrary value along the common edge. The edge load terms for moment and shear are defined in terms of a Fourier series.

$$F = \sum_{i=1}^{n} f_i \sin\left(\frac{i\pi\epsilon}{a}\right) \tag{11}$$

$$M = \sum_{i=1}^{n} m_i \sin\left(\frac{i\pi\epsilon}{a}\right) \tag{12}$$

where n is the number of harmonics choosen to compute the forces; and ϵ is the coordinate along the common edge.

The point load and moment terms are integrated along the common edge after multiplying with the unknown interactive forces, F and M. This is to ensure the continuous matching of deflection and slope perpendicular to the common edge. The $\triangle$ and $\bigcirc$ terms for each element are written with respect to the global axis system. When an element has two common edges (Fig. 2), the point force and moment at one free edge influences the slope and deflection terms at the other free edge, thus producing a coupling effect between the compatibility equations, and yielding the following equation:

Deflection or slope along the common edge produced by the external loading.
+ Deflection or slope along the common edge produced by the unit point load or moment at the common edge.
+ Deflection or slope along the common edge produced by the unit point load or moment at the elements other common edge or edges. (13)
= Adjacent elements contributions to the compatibility equation.

The compatibility equations are arranged into a global flexibility matrix. This is achieved by writing the compatibility equations for each harmonic and then assembling them in the flexibility matrix. The matrix representation for this operation is:

$$[A]\{B\} = \{C\} \tag{14}$$

where $[A]$ is the flexibility matrix composed of deflection and slope terms under unit loads; B is the unknown Fourier coefficients of the interactive forces along the common edge; and C is the deflection and slope terms produced by the external loads. Through standard inversion procedures $\{B\}$ can be written as,

$$\{B\} = [A]^{-1}\{C\}. \tag{15}$$

The final results are obtained by writing the deflection, slope, and moment equations, for each element. These results are evaluated by superimposing the effects of the arbitrary load, unit point loads, unit point moments, and the arbitrary line loads and moments.

$$W(x,y) = w^{al}(x,y) + F^1 w^{pl}(x,y) + M^1 w^{pm}(x,y) + F^2 w^{pl}(x,y) + M^2 w^{pm}(x,y) \tag{16}$$

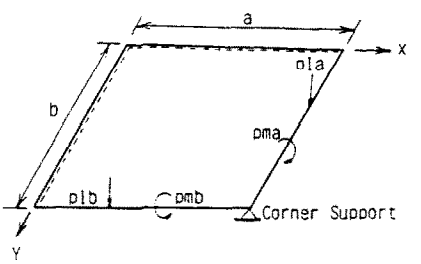

Fig. 2. Macro-element with two common edges.

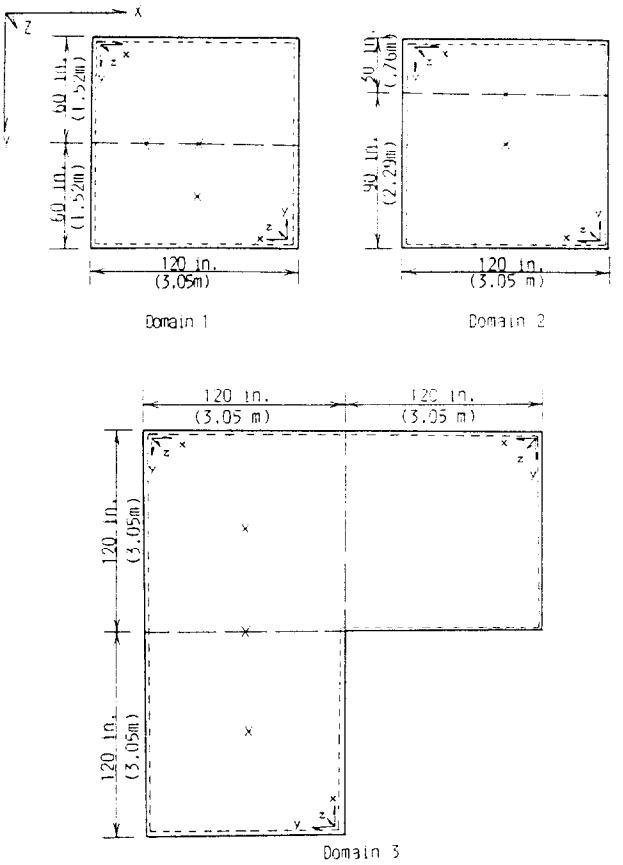

Fig. 3. Test domains.

where $w^{pl}(x, y)$ is the point load deflection; and $w^{pm}(x, y)$ is the point moment deflection.

The accuracy of the results is dependent on the number of terms summed.

To study the convergence obtained by the macro-approach and the accuracy of the results, three domains were modeled (Fig. 3). The convergence was studied from the first to the nth harmonics (sets of terms in the series). The macro-element results were compared to the results obtained by the classical and finite element approaches. Two rectangular domains were modeled; one domain with the common edge at the center of the domain, and the other with the common edge at the quarter point. The third domain, L-shaped, was modeled with the common edges perpendicular to each other.

In all domain studies, the following conditions were held constant:

E = 30,000,000 psi (2.109×10^{11} ksm)

Poisson's ratio = 0.30

and the domain was uniformly loaded at a magnitude of 0.208 psi (146.24 ksm) with all boundaries simply supported and 1" plate thickness.

RESULTS

For the first domain, convergence studies were performed for forces and displacements at the center of the domain, a quarter point along the common edge, and at the center of the macro-element. This results in the use of macro-elements with one common edge (macro-1-element). The results are listed in Tables 1–3.

In Domain 2, convergence studies were made at the center of the domain and the center of the common edge. The results are listed in Tables 4 and 5.

For Domain 3, convergence studies were conducted at the center of the corner element, a macro-element with two common edges (macro-2-element), center of common edge between the two macro-elements, and the center of macro-1-element. The results are listed in Tables 6–8.

Table 1. Domain 1—center of common edge

Harmonics Summed	Deflection—Inches	Slope (rad) X	Slope (rad) Y	Moment (in-lb) X	Moment (in-lb) Y
1	0.06482	0.0	0.0	-154.73	-145.56
2	0.06482	0.0	0.0	-154.34	-145.32
3	0.06362	0.0	0.0	-140.76	-142.30
4	-0.06359	0.0	0.0	-140.75	-142.27
5	0.06367	0.0	0.0	-143.85	-143.18
6	0.06367	0.0	0.0	-143.85	-143.21
Classical	0.06378	0.0	0.0	-143.67	-143.67

Table 2. Domain 1—1/4 point along common edge

Harmonics Summed	Deflection Inches	Slope (rad) X	Slope (rad) Y	Moment (in-lb) X	Moment (in-lb) Y
1	0.04584	0.00120	0.0	-109.42	-102.93
2	0.04545	0.00119	0.0	-109.13	-104.17
3	0.04612	0.00115	0.0	-118.88	-107.09
4	0.04609	0.00115	0.0	-118.85	-107.26
5	0.04606	0.00114	0.0	-116.67	-106.52
6	0.04605	0.00114	0.0	-116.67	-106.54
Classical	0.04613	0.00115	0.0	-116.52	-106.88

Table 3. Domain 1—center of macro-1-element

Harmonics Summed	Deflection Inches	Slope (rad) X	Slope (rad) Y	Moment (in-lb) X	Moment (in-lb) Y
1	0.04682	0.0	0.00118	-116.89	-122.24
2	0.04667	0.0	0.00115	-116.81	-122.81
3	0.04601	0.0	0.00114	-104.29	-115.33
4	0.04600	0.0	0.00114	-104.28	-115.37
5	0.04606	0.0	0.00114	-107.35	-116.75
6	0.04606	0.0	0.00114	-107.35	-116.77
Classical	0.04606	0.0	0.00115	-106.88	-116.52

Table 4. Domain 2—center of domain

Harmonics Summed	Deflection Inches	Slope (rad) X	Slope (rad) Y	Moment (in-lb) X	Moment (in-lb) Y
1	0.06502	0.0	0.0	-157.91	-154.99
2	0.06420	0.0	0.0	-154.06	-146.87
3	0.06348	0.0	0.0	-140.62	-142.18
4	0.06349	0.0	0.0	-140.79	-143.08
5	0.06355	0.0	0.0	-143.60	-143.00
6	0.06355	0.0	0.0	-143.59	-143.01
Classical	0.06378	0.0	0.0	-143.67	-143.67

Table 5. Domain 2—center of common edge

Harmonics Summed	Deflection Inches	Slope (rad) X	Slope (rad) Y	Moment (in-lb) X	Moment (in-lb) Y
1	0.04690	0.0	0.00117	-115.85	-118.30
2	0.04630	0.0	0.00114	-115.35	-120.24
3	0.04584	0.0	0.00114	-103.70	-114.52
4	0.04580	0.0	0.00114	-103.69	-114.52
5	0.04590	0.0	0.00114	-106.66	-115.48
Classical	0.04613	0.0	0.00115	-106.88	-116.52

Table 6. Domain 3—results at the center of the macro-2-element

Harmonics Summed	Deflection Inches	Slope (rad) X	Slope (rad) Y	Moment (in-lb) X	Moment (in-lb) Y
1	0.19076	0.00153	0.00153	-235.59	-235.59
2	0.18621	0.00141	0.00141	-233.14	-233.14
3	0.18090	0.00129	0.00129	-225.88	-225.88
4	0.17725	0.00131	0.00131	-223.83	-223.83
5	0.17396	0.00123	0.00123	-219.54	-219.54
6	0.17129	0.00122	0.00122	-217.85	-217.85

Table 7. Domain 3—results at the center of macro-1-element

Harmonics Summed	Deflection Inches	Slope (rad) X	Slope (rad) Y	Moment (in-lb) X	Moment (in-lb) Y
1	0.12804	-0.00153	0.00000	-135.45	-260.03
2	0.12577	-0.00139	-0.00001	-136.57	-256.47
3	0.12228	-0.00132	-0.00003	-126.86	-239.56
4	0.12046	-0.00133	-0.00002	-127.38	-236.99
5	0.11888	-0.00128	-0.00005	-127.12	-236.89
6	0.11754	-0.00126	-0.00004	-127.38	-234.95

Table 8. Domain 3—results at center of common edge between macro-elements

Harmonics Summed	Deflection Inches	Slope (rad) Type 1 X	Slope (rad) Type 1 Y	Slope (rad) Type 2 Y	Moment (in-lb) X	Moment (in-lb) Y
1	0.19572	0.00000	-0.00116	-0.00048	-352.35	-56.63
2	0.18806	0.00038	-0.00112	-0.00048	-339.29	-56.87
3	0.17995	0.00034	-0.00056	-0.00092	-314.05	-168.91
4	0.17525	0.00018	-0.00054	-0.00086	-311.64	-173.74
5	0.17205	0.00014	-0.00081	-0.00058	-289.59	-39.96
6	0.16878	0.00013	-0.00079	-0.00058	-283.12	-31.15
7	0 16600	0.00010	-0.00057	-0.00072	-320.95	-166.19
8	0.16358	0.00009	-0.00056	-0.00069	-320.98	-166.12
9	0.16122	0.00007	-0.00068	-0.00057	-255.04	-20.51
10	0.15927	0.00000	-0.00067	-0.00057	-250.36	-16.01
11	0.15773	0.00003	-0.00055	-0.00063	-336.77	-166.44
12	0.15610	0.00002	-0.00054	-0.00061	-337.60	-166.09

DISCUSSION

The behavior of a macro-1-element interacting with another macro-1-element was studied via Domains 1 and 2. The results at the center of the common edge in Domain 1 converged by the third harmonic. A comparison between the macro-element results for the third harmonic and the results obtained by the classical approach yielded: (1) 0.25% difference in deflection, (2) 0.0% difference in slope, (3) 2.03% difference in the x moment, (4) and 0.95% difference in the y moment. Similar results were obtained for the 1/4 point along the common edge (Table 2) and the center of the macro-1-element (Table 3).

Domain 2 was modeled with the common edge at the quarter point of the width. Again, the results obtained at the center of the domain converged to a high degree of accuracy by the third harmonic. Comparisons between the macro-approach and the classical approach for the third harmonic revealed a difference of: (1) 0.47% for deflection, (2) 2.12% for the x moment, and (3) 1.04% for the y moment.

The macro-approach maintained the deflected shape and a high degree of accuracy when the common edge did not pass through the center of the domain, thus illustrating that the results are virtually independent of the location of the common edge.

The macro-1-element converges rapidly, as illustrated by the results shown in Tables 1–5. As noted, the results obtained by the third harmonic are very close to the classical solution. Minimal changes in the results are obtained when the higher harmonics are summed. Therefore, nearly "exact" solutions are obtained by summing the first three harmonics.

The effects of two common edges at right angles is illustrated by Domain 3. Numerical convergence was examined at 3 points; (1) the center of the macro-2-element, (2) the center of the macro-1-element, and (3) the center of the common edge between the macro-elements.

The results at the center of the macro-2-element are presented in Table 6. After considering 4 harmonics there was a minimal change in the results for deflection and less than 2% change in moment per harmonic. A similar behavior was observed for the macro-1-element (Table 7).

A slow numerical convergence was achieved at the center of the common edge (Table 8). The deflection and x slope at the common edge converged at a predictable rate, i.e. monotonic convergence. However, the y slope at the common edge and the moments converged in a cyclic manner. The y slopes determined by the adjacent macro-elements are not equal. However, they converged towards each other as more harmonics were summed, and by the twelfth harmonic the slopes were approximately the same. Convergence studies revealed that little accuracy could be gained by summing more than twelve harmonics. However, it should be noted that the macro-1 and 2 elements predicted identical deflections, x and y moments, and x slopes at the common edge.

A study on the cyclic behavior of the slopes along the common edge in Domain 3 revealed that the results converged in sets of four harmonics. Two

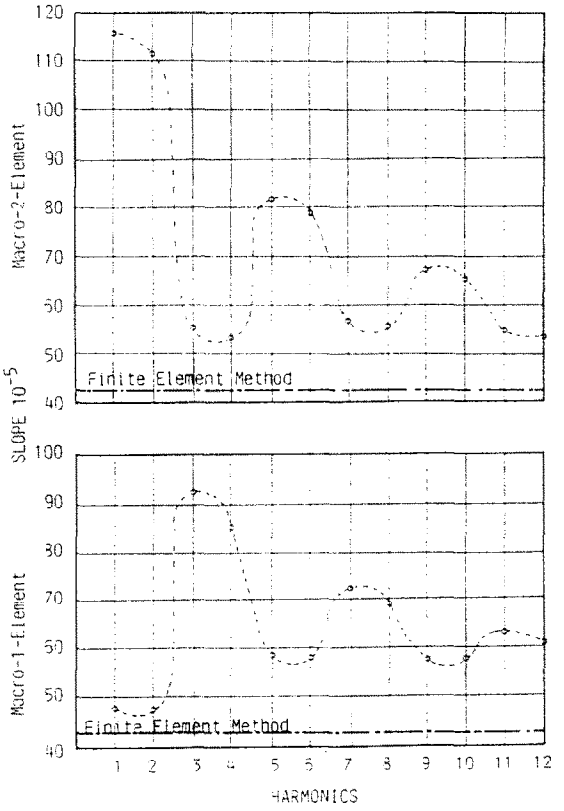

Fig. 4. Slope perpendicular to the common edge—Domain 3.

harmonics were lower and two were higher than the finite element values, resulting in the cyclic behavior (Fig. 4). As more harmonics are summed the difference between any two consecutive values usually decreased. The cyclic behavior becomes obvious by observing the slopes, where the elements predicted different slope values for the lower harmonics. For the first two harmonics, type-1-element predicted lower values than the type-2-element. For the next 2 harmonics, the reverse was true. For the second set of four values, the first 2 and next 2 harmonics of type-1-element had higher and lower values, respectively, than the type-2-element. As more harmonics were summed, the slope values alternated, i.e. keeping the sum of the slopes at a nearly constant magnitude, (Fig. 4) and converged toward a single term. By observing the first three sets of harmonics (fourth, eighth, and twelfth) a rapid convergence of results was noted.

In general, the macro-approach predicted numerically larger deflections, slopes, and moments than the ones obtained by the finite element method.

The discrepancy between the results obtained by the macro-approach and finite element method may be explained by noting the following:

(1) The results obtained for Domains 1 and 2 are virtually the same as the classical solution values. It has been shown that for the third harmonic the macro-elements results for deflection and moment are within 2% of the classical solutions. The "exact" solution to the biharmonic equation is obtained by the classical approach. Therefore this shows that the macro-approach obtains nearly "exact" solutions for the macro-1-domains examined.

(2) There is a uniform difference in deflection between the results obtained by the macro-approach and finite element method at the center of the macro-1-element, the center of the macro-2-element, and the center of the common edge. Due to the fact that the macro-1-element is very reliable and the deflection results obtained with the type-2-element are uniformly larger tends to demonstrate that the macro-2-element has predicted reliable results.

(3) The finite elements are stiffer, as established by many researchers[3, 9], therefore, they tend to reduce the magnitude of the displacements.

(4) A comparison between the domains revealed that the domain with the macro-2-element did not converge as rapidly as the domains with the macro-1-elements. The macro-2-element is more complex (for two adjacent sides are free) and the slope converges at a slower rate along the free edge. Since the slope is used in writing the compatibility equations, the slower convergence affected the macro-approach's results.

CONCLUSIONS

In summmary, the macro-approach has advanced the state of the art in the field of plate bending analysis by satisfying the natural and forced boundaries along all edges. The following contributions are made by the macro-approach:

(1) The proposed method deals with more complex shape functions with minimal input effort than the classical finite element method, wherein the shape functions are relatively simple and the input efforts are involved.

(2) Highly accurate and reliable macro-elements were developed. The results obtained by the macro-elements virtually agreed with the classical solutions. For the rectangular domains, the deflection converged to within 2% of the classical results by the third harmonic.

(3) The macro-approach permits the determination of the deflection and moment values at any point in the domain and on the boundary. This is an advantage over the finite element method, where results are usually calculated at the node points.

(4) Compatibility of deflection, slope, and moment was obtained with the aid of a continuous function along the common edge. This is an advancement over the classical finite element method, where compatibility is only maintained at the node points.

REFERENCES

1. V. C. Chaudhary, Analysis of plates with various shapes and boundaries. Ph.D., West Virginia University (1977).
2. H. Farran, Analysis of stiffened plate structures of various shapes and boundaries. Ph.D., West Virginia University (1981).
3. R. H. Gallagher, *Finite Element Analysis Fundamentals*. Prentice-Hall, Englewood Cliffs, New Jersey (1975).
4. H. GangaRao, A discrete field macro approach to the analysis of latticed structures. Masters Thesis, North Carolina State University (1967).
5. H. GangaRao and V. C. Chaudhary, Macro approach for ribbed and grid plate systems. *J. Engng Mech. Div., Proc. Am. Soc. Civil Engrs* (1975).
6. R. M. Gutkowski, Finite panel analysis of orthotropic plate systems. *J. Structural Div., ASCE* **103**, 2211–2223 (1977).
7. R. M. Gutkowski and C. K. Wang, Continuous plate analysis by finite panel method. *J. Structural Div., ASCE* **102**, 629–643 (1976).
8. T. J. Parsons, Plate bending analysis by macro flexibility approach. Ph.D., West Virginia University (1981).
9. R. Szilard, *Theory and Analysis of Plates and Classical and Numerical Methods*. Prentice-Hall, Englewood Cliffs, New Jersey (1974).
10. T. Wah, Elastic quadrilateral plates. *Comput. Structures* **10**, 457–466.